Nuclear Physics B324 (1989) 684–714
North-Holland, Amsterdam

THE ROLE OF A KERNEL IN COMPLEX LANGEVIN SYSTEMS*

H. OKAMOTO[1], K. OKANO, L. SCHÜLKE and S. TANAKA[1]

FB Physik, Universität-Gesamthochschule Siegen, D-5900 Siegen, Fed. Rep. Germany
[1]*Dept. of Physics, Waseda University, Tokyo 169, Japan*

Received 8 September 1988
(Revised 13 March 1989)

The role of a kernel in the complex Langevin equation is investigated in detail theoretically and numerically. We have applied this scheme to Minkowski stochastic quantization and the numerical simulation of simple polynomial models. It is shown that the kernel can stabilize the solution of the Langevin equation. Solutions in different Riemann sheets are found and criteria are given to select the physical one.

1. Introduction

Monte Carlo simulation has been extensively used in simulating lattice gauge theories. This is, however, only possible for systems with real actions in euclidean space-time. On the other hand, complex actions are met in several cases. Examples are QCD in the charged sector [1], with fermion determinant with non-zero chemical potential [2], or effective actions with topological terms [3]. Moreover, the simulation in Minkowski space instead of euclidean space is another interesting example. In these cases normal Monte Carlo simulation is said to be irrelevant, see, e.g., ref. [4].

Here complex Langevin simulation [5,6] has recently taken hold. The Langevin equation as a differential equation can be solved directly, independent of the fact whether the drift term is real or complex. Actually, however, there are some examples where this naïve expectation fails because (a) we encounter blow-up solutions [7,8], or because (b) the updated field configurations are sometimes stuck in only a part of the configuration space [9].

In case (a) where one encounters blow-up solutions, stable results can be obtained if those solutions are thrown away and the corresponding updates are repeated. The results, however, can sometimes be wrong, making this method unreliable. In ref. [7] it was discussed that the positivity of the real part of the eigenvalue of the

*Supported in part by the German Bundesministerium für Forschung und Technologie (BMFT).

Fokker–Planck hamiltonian controls the convergence. Concerning problem (b), i.e., violation of the ergodic property, some attempt has been made [10] to overcome it but no general solution has been reached so far.

The idea of using a kernel in Langevin equations has been studied, e.g., in the context with stochastic quantization of fermions [11], or overcoming critical slowing down in numerical simulation [12].

The role of the kernel in the *complex* Langevin equation, however, has so far not been investigated systematically*, while a kernel has been used to stabilize the system in Langevin perturbation in Minkowski space [14, 15]. Especially in connection with point (a) above it is obvious that the introduction of a kernel should be very important, since it affects the eigenvalues of the Fokker–Planck hamiltonian, which control the convergence property of the solution of the Langevin equation.

In this paper, the role of the kernel in the complex Langevin system is studied, in particular in connection with item (a) discussed above. Our main results are:

(i) The kernel changes the eigenvalue spectrum of the Fokker–Planck hamiltonian which indeed can be adjusted to stabilize the system. The mechanism as to how this works is discussed through explicitly solving the Fokker–Planck equation in simple cases.

(ii) We can control the convergence of Minkowski stochastic quantization by the kernel. The convergence is not governed by the small parameter $i\epsilon$.

(iii) If the quantum mechanical average of a certain physical quantity is a multi-valued function of the parameters in the action, the kerneled Langevin equation gives the results in all branches. This means that we might also suffer from the problem of stable but unphysical solutions. Within the simple models treated here we could, however, give criteria to choose that kernel which leads to the physical result, or we can give criteria for the case that no stable physical solution is expected.

There remain, of course, open questions to be solved in future work: In numerical simulation, we have restricted our discussion to simple zero-dimensional field theoretical models. There will still be a big step towards a realistic field theory, e.g., it is not a priori clear what kind of kernel can settle the convergence problem and avoid the unphysical solutions in such a case. For tackling this problem we think, however, that the precise knowledge about the behaviour of the simple models will surely be helpful. Concerning the other problem referred to in item (b), it is an open and interesting question whether the degree of the kernel can help to recover the ergodic property of the complex Langevin simulation, which is known to be lost in certain interesting physical models. To attack this problem it will surely be inevitable to introduce at least field-dependent kernels.

* After this paper was completed, we became aware of a paper by B. Söderberg [13] in which a theoretical analysis about the role of the kernel in the complex Langevin equation is given. Some of our results in sect. 3 and his results overlap.

The paper is organized as follows: In sect. 2 the theoretical framework for the kerneled complex Langevin system is described. In sect. 3 the complex gaussian model is discussed in some detail, solving the Fokker–Planck equation exactly and including a numerical analysis. The above arguments are applied to the case of a neutral scalar field in the Minkowski space in sect. 4. In sect. 5 we discuss the role of a kernel in complex Langevin simulation for the special cases of power and polynomial actions. Finally, sect. 6 contains the conclusion and discussions.

2. Complex Langevin equation with a kernel

In this section we would like to review briefly the theoretical framework of a system described by a complex Langevin equation, where we introduce a complex kernel K which will be useful for stabilizing the system. Concerning a more general discussion of the complex kernel using the terminology of the geometry in the space of the dynamical variables see ref. [13].

Let us consider the simple example of one degree of freedom, the action being $S(x)$, where x is real valued but S itself is complex. In order to quantize the system we consider a stochastic process in the complex z-plane. The Langevin equation with kernel $K(z)$ can be written in the form

$$\dot{z}(t) = -K\frac{\partial S}{\partial z} + \frac{\partial K}{\partial z} + \xi(z,t), \tag{2.1a}$$

where the dot stands for the derivative with respect to the fictitious time t, and the noise term ξ satisfies

$$\langle \xi(t) \rangle = 0, \qquad \langle \xi(t), \xi(t') \rangle = 2K(z)\delta(t-t'). \tag{2.1b}$$

The simplest choice satisfying eq. (2.1b) by use of a real gaussian white noise η is

$$\xi(z,t) = \sqrt{K(z)}\,\eta(t), \tag{2.2a}$$

$$\langle \eta(t) \rangle = 0; \qquad \langle \eta(t), \eta(t') \rangle = 2\delta(t-t'). \tag{2.2b}$$

The Langevin equation (2.1) can be rewritten using two real variables x, y as

$$\dot{x} = -\mathrm{Re}\left(K\frac{\partial S}{\partial z} - \frac{\partial K}{\partial z} \right) + \mathrm{Re}(\xi), \tag{2.3a}$$

$$\dot{y} = -\mathrm{Im}\left(K\frac{\partial S}{\partial z} - \frac{\partial K}{\partial z} \right) + \mathrm{Im}(\xi). \tag{2.3b}$$

This stochastic process can also be described by the corresponding real probability

distribution $P(x, y: t)$, which obeys the Fokker–Planck equation

$$\dot{P}(x, y: t) = -H_{\mathrm{FP}} P(x, y: t), \tag{2.4a}$$

$$H_{\mathrm{FP}} = -\frac{\partial^2}{\partial x^2}(\mathrm{Re}\sqrt{K})^2 - \frac{\partial^2}{\partial y^2}(\mathrm{Im}\sqrt{K})^2 - 2\frac{\partial^2}{\partial x\,\partial y}(\mathrm{Re}\sqrt{K})(\mathrm{Im}\sqrt{K})$$
$$+\frac{\partial}{\partial x}\left[\mathrm{Re}\left(K\frac{\partial S}{\partial z} - \frac{\partial K}{\partial z}\right)\right] + \frac{\partial}{\partial y}\left[\mathrm{Im}\left(K\frac{\partial S}{\partial z} - \frac{\partial K}{\partial z}\right)\right]. \tag{2.4b}$$

For a derivation of this equation one uses the formula

$$\langle f(x+iy)\rangle = \int \mathrm{d}x\,\mathrm{d}y\, P(x, y: t) f(x+iy). \tag{2.5}$$

together with the Langevin equations (2.3), where f represents a certain physical quantity.

The interpretation of the thermal equilibrium limit of the above real Fokker–Planck distribution $P(x, y: t)$ itself is not obvious. In order to extract its physical content, one introduces [5, 8] the complex valued distribution $P(x: t)$ of a real parameter x by the formula

$$\iint \mathrm{d}x\,\mathrm{d}y f(x+iy) P(x, y: t) = \int \mathrm{d}x f(x) P(x: t). \tag{2.6}$$

Through this equation we get the complex valued Fokker–Planck equation controlling the time development of the distribution $P(x: t)$

$$\dot{P}(x: t) = -H_{\mathrm{FP}}(x) P(x: t), \tag{2.7a}$$

$$H_{\mathrm{FP}}(x) = -\frac{\partial}{\partial x} K(x)\left(\frac{\partial}{\partial x} + \frac{\partial S}{\partial x}\right). \tag{2.7b}$$

The physical contents of the complex Langevin equation (2.1) can be discussed through this equation. If the real part of the Fokker–Planck hamiltonian is positive semi-definite [7] or can be made positive semi-definite by choosing a suitable kernel $K(z)$ in eq. (2.7), in thermal equilibrium the distribution $P(x: t)$ tends to the desired limit, i.e.,

$$\mathrm{Re}\, H_{\mathrm{FP}}(x) > 0, \qquad P(x: t) \to P_{\mathrm{eq}}(x) = \mathrm{e}^{-S(x)}. \tag{2.8}$$

In solving the Langevin equation (2.1), one gets a set of complex numbers, $\{z = x + iy\}$, whose real and imaginary parts are distributed according to $P(x, y: t)$.

Corresponding to this set we can calculate a set of $\{f(z)\}$ and its average $\langle f(z)\rangle$. From the above considerations it is now clear, that the average calculated in this way has the meaning of a quantum mechanical average of f over the complex measure $\exp\{-S(x)\}$ through eqs. (2.6) and (2.8).

Furthermore, compared to the usual treatment, we have an additional adjustable factor $K(x)$ in the Fokker–Planck hamiltonian, which we can use to improve the convergence properties.

3. The complex gaussian model

As the simplest example we like to consider the complex gaussian model,

$$S = \frac{\sigma}{2}x^2, \quad \text{with } \sigma = a + ib. \tag{3.1a}$$

We will discuss this system for σ within the full complex plane. This includes the case of a Minkowski path integral (σ purely imaginary), and the bottomless system ($\mathrm{Re}(\sigma) < 0$). As is well known, the average $\langle x^2\rangle$ can be calculated, for $\mathrm{Re}(\sigma) > 0$, analytically,

$$\langle x^2\rangle = \frac{1}{\sigma}. \tag{3.1b}$$

The result can be continued into the entire complex plane. Although the physical interpretation of this continuation is still under discussion, it is used sometimes, e.g. in the quantization of the gravitational field [16]. Here we want to show the efficiency of a suitably chosen kernel to improve the convergence properties or, in some cases, to change them completely, i.e., the kernel allows for a solution where the solution of the naïve equation does not converge.

In this case we can restrict ourselves to the use of a constant kernel $K(x) = K$ only. The Langevin equation (2.1) then reads

$$\dot{z} = -K\sigma z + \sqrt{K}\eta. \tag{3.2}$$

The complex valued Fokker–Planck hamiltonian which controls the convergence properties of the system through its positive semi-definiteness, is given by

$$H(x) = KH_0(x), \qquad H_0(x) = -\frac{\partial}{\partial x}\left[\frac{\partial}{\partial x} + \frac{\partial S}{\partial x}\right]. \tag{3.3}$$

The result of a calculation of the eigenvalues E_n of this Fokker–Planck hamiltonian, $Hf_n = E_n f_n$, is

$$E_n = nK\sigma. \tag{3.4}$$

In the present case the Langevin equation can easily be solved, and we can calculate the expectation value for any physical quantity exactly. However, it is very interesting to show the results of a numerical analysis in order to check the effectivity of the kernel in systems described by a complex Langevin equation, in particular in connection with the positive semi-definiteness of the above Fokker–Planck hamiltonian (3.3), or (3.4).

3.1. RESULT OF THE NUMERICAL SIMULATION

Let us start to discuss the naïve Langevin equation first, i.e., that with $K = 1$. Looking at the eigenvalue equation (3.4) one can see that in this case the positivity condition (2.8) will be satisfied, if only $\mathrm{Re}(\sigma) > 0$. On the other hand, if $\mathrm{Re}(\sigma) < 0$, we cannot expect to get a reasonable result. To check these expectations, we have performed numerical calculations for

$$\sigma = \mathrm{e}^{n(\pi/6)i}, \quad n = 0, \ldots, 11. \tag{3.5}$$

We have used a simple Euler discretization of eq. (3.2) with eq. (2.2), with discretization step $\mathrm{d}t = 0.01$. A sample of 64 runs, each with 2000 updates, was taken to calculate the mean value and the statistical error.

In fig. 1a we show the result of a numerical calculation of $\langle x^2 \rangle$ in comparison with eq. (3.1b). As one expects, for $\mathrm{Re}(\sigma) > 0$ the numerical results agree with those calculated analytically within the error limits. For purely imaginary σ the error bar has increased appreciably. Although the result is not far from the predicted value, a more careful analysis, taking more updates into account, shows that it is very unstable due to the fact that the system is not thermalized. This is even more the case for $\mathrm{Re}(\sigma) < 0$, where the numerical analysis never gets a reasonable result, but always ends in blow up solutions.

In contrast to that, fig. 1b shows agreement of the numerical data with the analytic solution, eq. (3.1b), in the entire complex plane. Here we have used a kernel

$$K = \sigma^*, \tag{3.6}$$

which makes the eigenvalues of the Fokker–Planck hamiltonian (3.4) always positive, independent of the choice of σ. This ensures the convergence of the complex Langevin system to the desired thermal equilibrium limit, as was mentioned in eq. (2.8).

Although the numerical simulation of this simple model seems to be rather trivial, it can serve as an intuitive example to show the effect of the kernel. It is quite interesting to mention, that from the kerneled Langevin equation we get a sample of $\{z_1, z_2, \ldots\}$, which gives us the average $\langle z^2 \rangle$ coinciding with that obtained by an analytical calculation even for $\mathrm{Re}(\sigma) < 0$, where the result $1/\sigma$ is only defined in the sense of analytic continuation and has no real physical meaning (bottomless action).

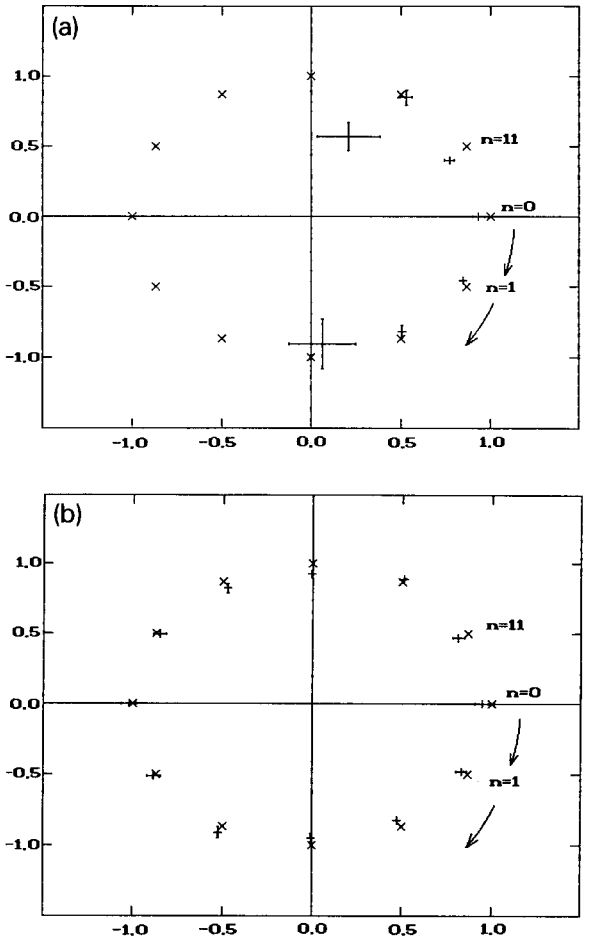

Fig. 1. (a) The average $\langle z^2 \rangle$ for the complex gaussian model, $S = \sigma x^2/2$, with $\sigma = \exp\{n\pi i/6\}$. The points (+) give the results of a numerical simulation including the error, while (×) shows the analytical results $1/\sigma$. No kernel has been used in the simulation. (b) Similar to (a), however, with kernel adjusted as $K = \sigma^*$.

3.2. ANALYTIC SOLUTION OF THE FOKKER–PLANCK EQUATION

The role the kernel plays has been clarified by numerical methods in the previous section. It is now interesting to investigate it from the analytical point of view. As was mentioned already, the kerneled complex Langevin equation has also been analyzed theoretically in ref. [13]. In the case of the complex gaussian model, the form of the real valued Fokker–Planck distribution $P(x, y: t)$ at the thermal equilibrium limit $t \to \infty$ has been given there. It is, however, still very interesting and intuitive to see the exact form of the solution for $P(x, y: t)$ at finite t to show the relation between the kernel and the relaxation of the system to thermal

equilibrium. This can be done following ref. [17], where the naïve Langevin equation for the gaussian model without kernel has been treated. Here we give the result of the corresponding analysis with a kernel, referring for the details to the appendix.

The Fokker–Planck equation to be solved is given in eq. (2.4), with action S given in eq. (3.1). We take a constant complex kernel $\sqrt{K} = \alpha + i\beta$, with real α, β, and introduce the real parameters A, B by $A + iB = K\sigma$. In this case the Fokker–Planck equation reads

$$\dot{P}(x, y : t) = -H_{\mathrm{FP}}(x, y)\, P(x, y : t), \tag{3.7a}$$

$$H_{\mathrm{FP}}(x, y) = -\left(\alpha^2 \frac{\partial^2}{\partial x^2} + \beta^2 \frac{\partial^2}{\partial y^2} + 2\alpha\beta \frac{\partial^2}{\partial x\, \partial y} + \frac{\partial}{\partial x}(Ax - By) + \frac{\partial}{\partial y}(Bx + Ay) \right). \tag{3.7b}$$

The solution of the above Fokker–Planck equation, with initial distribution $P_0(x, y)$ is given by (for the details of the derivation see the appendix):

$$P(x, y : t) \propto \int \mathrm{d}x'\, \mathrm{d}y' \exp\left\{ \frac{G_3 H_1^2 - 2G_2 H_1 H_2 + G_1 H_2^2}{2(G_1 G_3 - G_2^2)} \right\} P_0(x', y'), \tag{3.8}$$

where

$$G_1 = \tfrac{1}{2}(u + w) + \tfrac{1}{2}\mathrm{e}^{-2At}(-u\cos(2Bt) - v\sin(2Bt) - w), \tag{3.9a}$$

$$G_2 = \tfrac{1}{2}v + \tfrac{1}{2}\mathrm{e}^{-2At}(u\sin(2Bt) - v\cos(2Bt)), \tag{3.9b}$$

$$G_3 = \tfrac{1}{2}(-u + w) + \tfrac{1}{2}\mathrm{e}^{-2At}(u\cos(2Bt) + v\sin(2Bt) - w), \tag{3.9c}$$

$$H_1 = -i(x - \mathrm{e}^{-At}(x'\cos(Bt) + y'\sin(Bt)), \tag{3.9d}$$

$$H_2 = -i(y - \mathrm{e}^{-At}(-x'\sin(Bt) - y'\cos(Bt)), \tag{3.9e}$$

with

$$u + iv = \sigma^{-1} = \frac{1}{a^2 + b^2}(a - ib), \qquad w = \frac{\alpha^2 + \beta^2}{A} = \frac{|K|}{A}. \tag{3.10a, b}$$

These formulae explicitly show that the relaxation of the real Fokker–Planck distribution is controlled by $A = \mathrm{Re}(K\sigma)$ and we can choose K suitably to ensure convergence. In the case that we choose $A > 0$, all of the terms are convergent for $t \to \infty$. In particular the x', y'-dependence within the exponential factor (integration kernel) disappears. This makes the thermal equilibrium form of the

Fokker–Planck distribution independent of the initial distribution. It is given by

$$P_{\mathrm{eq}}(x, y) \propto \exp\left\{ \frac{1}{w^2 - u^2 - v^2} \left(-(w-u)x^2 + 2vxy - (w+u)y^2 \right) \right\}. \quad (3.11)$$

As was mentioned this thermal equilibrium distribution has also been obtained in ref. [13]. Using eq. (2.6) we can get the thermal equilibrium form for the complex valued Fokker–Planck distribution as

$$P_{\mathrm{eq}}(x) = \int \mathrm{d}y\, \mathrm{e}^{-iy\partial/\partial x} P_{\mathrm{eq}}(x, y) \propto \mathrm{e}^{-(\sigma/2)x^2}. \quad (3.12)$$

This distribution is exactly what we expected from the beginning. It is now clear from this simple example that the introduction of a kernel in fact works to force the system to converge.

Here we would like to give explicitly the real valued Fokker–Planck distribution in the limit of thermal equilibrium for the two limiting cases $S = -(|a|/2)x^2$ (bottomless case), and $S = i(b/2)x^2$ (Minkowski case), both with a phase rotating kernel

$$K = \mathrm{e}^{-i\theta}. \quad (3.13)$$

With the use of the abbreviations A_1, A_2, A_3 (compare eq. (3.11))

$$P_{\mathrm{eq}}(x, y) = \exp\left\{ -A_1 x^2 - A_2 xy - A_3 y^2 \right\}, \quad (3.14)$$

we get for the bottomless case,

$$A_1 = \frac{|a|(-\cos\theta)}{1 + \cos\theta}, \qquad A_2 = 0, \qquad A_3 = \frac{|a|(-\cos\theta)}{1 - \cos\theta}, \quad (3.15)$$

and for the Minkowski case,

$$A_1 = \frac{b \sin\theta}{\cos^2\theta}, \qquad A_2 = 2b \tan^2\theta, \qquad A_3 = \frac{b \sin\theta}{\cos^2\theta}. \quad (3.16)$$

We would like to note that the factors $-|a|\cos\theta$ in eq. (3.15) and $b\sin\theta$ in eq. (3.16) are nothing but $\mathrm{Re}(K\sigma)$ and have therefore to be taken positive. Thus in both cases the distribution (3.14) is well defined. As can be understood from eq. (3.12), the dependence of $P(x, y)$ on the kernel disappears when we calculate the expectation value of any physical quantity f using eq. (2.5).

Finally we would like to note that from eq. (3.12) together with the above distribution (3.14) we get for $\theta = \pi$ for the bottomless case

$$P_{\mathrm{eq}}(x) \sim \int \mathrm{d}y\, \mathrm{e}^{-(|a|/2)y^2}\, \delta(x - iy), \tag{3.17a}$$

and for the Minkowski case for $\theta = \pi/2$

$$P_{\mathrm{eq}}(x) \sim \int \mathrm{d}y\, \mathrm{e}^{-|b|y^2}\, \delta\left(y + \frac{1+i}{2}x\right). \tag{3.17b}$$

As one can see from these formulas, the distribution in y is well defined, i.e. $\propto \exp\{-|\gamma|y^2\}$. This might give us the key for an understanding of the fact that the Langevin equation with a kernel is able to give a result in cases where the original distribution is ill-defined. These formulas might be useful also for Monte Carlo simulation of those systems.

4. Neutral scalar field in the Minkowski space

In this section we apply our discussion in the previous section to the formulation of the stochastic quantization in the four-dimensional Minkowski space [18, 19]. For simplicity we focus on the neutral free scalar field. The Minkowski action is given by

$$S[\phi] = \int \mathrm{d}^4x\, \tfrac{1}{2}\left\{\partial^\mu\phi(x)\, \partial_\mu\phi(x) - (m^2 - i\epsilon)\phi^2(x)\right\}, \tag{4.1}$$

where ϵ is a small positive constant which is set equal to zero after all calculations have been performed. In the naïve Minkowski stochastic quantization scheme where $K(x) = \delta^4(x)$, the relaxation time is proportional to $1/\epsilon$ [19, 20]. Such a scheme is not suitable for application to numerical simulations. Moreover, when such a scheme is applied to gauge field theories, introduction of ϵ breaks gauge invariance. For these reasons it is important to formulate a stochastic quantization scheme in which the relaxation time is not governed by the value of ϵ. The construction of such a scheme becomes possible by introduction of a proper kernel.

We adopt the following Langevin equation with a kernel $K(x)$.

$$\dot{\phi}(x,t) = i\int \mathrm{d}^4y\, K(x-y)\left.\frac{\delta S[\phi]}{\delta\phi(y)}\right|_{\phi(y)\to\phi(y,t)} + \xi(x,t), \tag{4.2a}$$

where the random variable $\xi(x,t)$ is required to satisfy the statistical properties

$$\langle\xi(x,t)\rangle = 0, \qquad \langle\xi(x,t)\xi(x',t')\rangle = 2K(x-x')\delta(t-t'). \tag{4.2b}$$

We choose our kernel in the following form:

$$K(x) = \int \frac{d^4p}{(2\pi)^4} \tilde{K}(p) e^{-ipx}, \tag{4.3a}$$

with

$$\tilde{K}(p) = \frac{iA(p)}{p^2 - m^2 + i\epsilon}. \tag{4.3b}$$

In eq. (4.3b) $A(p)$ is assumed to be a real, positive and even function of p:

$$A(p) > 0, \qquad A(p) = A(-p). \tag{4.4}$$

This form of the kernel has been used in ref. [14] to discuss the relation between stochastic diagrams and Feynman diagrams in Minkowski space.

Let us investigate our stochastic process (4.2) in momentum space. The momentum representation of ϕ is defined as

$$\phi(x,t) = \int \frac{d^4p}{(2\pi)^2} \phi(p,t) e^{-ipx}. \tag{4.5}$$

The simplest definition of $\xi(x,t)$ satisfying eq. (4.2b) is

$$\xi(x,t) = \int \frac{d^4p}{(2\pi)^2} \xi(p,t) e^{-ipx}, \tag{4.6}$$

$$\xi(p,t) = \sqrt{\tilde{K}(p)}\,\eta(p,t) = [\alpha(p) + i\beta(p)]\eta(p,t), \tag{4.7}$$

where $\alpha(p)$ and $\beta(p)$ are real, and $\eta(p,t)$ is the gaussian white noise satisfying

$$\langle \eta(p,t) \rangle = 0, \qquad \langle \eta(p,t)\eta(p',t') \rangle = 2\delta^4(p+p')\delta(t-t'). \tag{4.8}$$

Then eq. (4.2) can be rewritten as the Langevin equation for $\phi(p,t)$ in the form

$$\dot{\phi}(p,t) = -A(p)\phi(p,t) + \xi(p,t), \tag{4.9a}$$

$$\langle \xi(p,t) \rangle = 0, \qquad \langle \xi(p,t)\xi(p',t') \rangle = 2\tilde{K}(p)\delta^4(p+p')\delta(t-t'). \tag{4.9b}$$

The drift term of eq. (4.9) clearly exhibits that the relaxation time is $1/A(p)$ and therefore, as desired, not affected by ϵ.

The Langevin equation (4.9) can be decomposed into the following set of Langevin equations

$$\dot{\phi}_{\mathrm{R}}(p,t) = -A(p)\phi_{\mathrm{R}}(p,t) + \alpha(p)\eta(p,t), \tag{4.10a}$$

$$\dot{\phi}_{\mathrm{I}}(p,t) = -A(p)\phi_{\mathrm{I}}(p,t) + \beta(p)\eta(p,t), \tag{4.10b}$$

where $\phi_{\mathrm{R}}(p,t)$ and $\phi_{\mathrm{I}}(p,t)$ are the momentum representations of the real and imaginary part of $\phi(x,t)$. Note that $\phi(p,t) = \phi_{\mathrm{R}}(p,t) + i\phi_{\mathrm{I}}(p,t)$, but $\phi_{\mathrm{R}}(p,t) \neq \mathrm{Re}\,\phi(p,t)$ and $\phi_{\mathrm{I}}(p,t) \neq \mathrm{Im}\,\phi(p,t)$. In deriving eq. (4.10), we have used the fact that $f(p) + ig(p) = 0$ is equivalent to $f(p) = g(p) = 0$ if $f^*(p) = f(-p)$ and $g^*(p) = g(-p)$ are satisfied. The real-valued Fokker–Planck equation equivalent to (4.10) is

$$\dot{P}[\phi_{\mathrm{R}}, \phi_{\mathrm{I}}: t] = -H_{\mathrm{FP}}[\phi_{\mathrm{R}}, \phi_{\mathrm{I}}]P[\phi_{\mathrm{R}}, \phi_{\mathrm{I}}: t], \tag{4.11a}$$

$$\begin{aligned} H_{\mathrm{FP}}[\phi_{\mathrm{R}}, \phi_{\mathrm{I}}] = -\int \mathrm{d}^4p \Bigg[& \alpha^2(p)\frac{\delta^2}{\delta\phi_{\mathrm{R}}(p)\delta\phi_{\mathrm{R}}(-p)} + \beta^2(p)\frac{\delta^2}{\delta\phi_{\mathrm{I}}(p)\delta\phi_{\mathrm{I}}(-p)} \\ & + 2\alpha(p)\beta(p)\frac{\delta^2}{\delta\phi_{\mathrm{R}}(p)\delta\phi_{\mathrm{I}}(-p)} + \frac{\delta}{\delta\phi_{\mathrm{R}}(p)}A(p)\phi_{\mathrm{R}}(p) \\ & + \frac{\delta}{\delta\phi_{\mathrm{I}}(p)}A(p)\phi_{\mathrm{I}}(p)\Bigg]. \end{aligned} \tag{4.11b}$$

This Fokker–Planck equation can be solved in the same way as in sect. 3. The normalized asymptotic distribution is

$$\begin{aligned} P_{\mathrm{eq}}[\phi_{\mathrm{R}}, \phi_{\mathrm{I}}] &\equiv \lim_{t\to\infty} P[\phi_{\mathrm{R}}, \phi_{\mathrm{I}}: t] \\ &= \frac{1}{N}\exp\left\{-\int \mathrm{d}^4p\,\frac{A(p)}{2\alpha^2(p)}\phi_{\mathrm{R}}(p)\phi_{\mathrm{R}}(-p)\right\}\delta\left(\frac{\beta}{\alpha}\phi_{\mathrm{R}} - \phi_{\mathrm{I}}\right), \end{aligned} \tag{4.12a}$$

$$N \equiv \int \mathscr{D}\phi_{\mathrm{R}} \exp\left\{-\int \mathrm{d}^4p\,\frac{A(p)}{2\alpha^2(p)}\phi_{\mathrm{R}}(p)\phi_{\mathrm{R}}(-p)\right\}. \tag{4.12b}$$

Note that P_{eq} is normalizable as long as $A(p)$ is positive. This asymptotic distribution makes sense even in the limit $\epsilon \to 0$, while in the naïve scheme where $K(x) = \delta^4(x)$ the asymptotic distribution becomes a constant in this limit [19].

Any expectation value can be calculated by differentiating the following generating functional:

$$Z[J_R, J_I] = \int \mathscr{D}\phi_R \mathscr{D}\phi_I P_{eq}[\phi_R, \phi_I] \exp\left\{ \int d^4p \, [J_R(p)\phi_R(p) + J_I(p)\phi_I(p)] \right\}$$

$$= \exp\left\{ \int d^4p \, \frac{\alpha^2(p)}{2A(p)} J(p)J(-p) \right\}, \tag{4.13a}$$

with

$$J(p) = J_R(p) + \frac{\beta(p)}{\alpha(p)} J_I(p). \tag{4.13b}$$

For example we can obtain the correct propagator as

$$\langle \phi(p_1)\phi(p_2) \rangle = \delta^4(p_1 + p_2) \frac{\tilde{K}(p_1)}{A(p_1)} = \delta^4(p_1 + p_2) \frac{i}{p_1^2 - m^2 + i\epsilon}. \tag{4.14}$$

For any physical quantity $F[\phi]$ the correct quantum expectation value in the Minkowski space can be obtained. In fact, it is easy to show that

$$\langle F[\phi] \rangle = \int \mathscr{D}\phi_R \mathscr{D}\phi_I F[\phi_R + i\phi_I] P_{eq}[\phi_R, \phi_I] = \frac{\int \mathscr{D}\phi_R \, F[\phi_R] e^{iS[\phi_R]}}{\int \mathscr{D}\phi_R \, e^{iS[\phi_R]}} \tag{4.15}$$

through explicit calculation by using eq. (4.12).

The existence of a unique equilibrium distribution is also suggested from the following analysis of a Fokker–Planck hamiltonian. The Langevin equation (4.10) can be rewritten as

$$\dot{\phi}_1(p, t) = -A(p)\phi_1(p, t), \tag{4.16a}$$

$$\dot{\phi}_2(p, t) = -A(p)\phi_2(p, t) + \sqrt{2}\eta(p, t), \tag{4.16b}$$

with

$$\phi_1(p, t) = \frac{1}{\sqrt{2}} \left\{ \frac{\phi_R(p, t)}{\alpha(p)} - \frac{\phi_I(p, t)}{\beta(p)} \right\}, \tag{4.17a}$$

$$\phi_2(p, t) = \frac{1}{\sqrt{2}} \left\{ \frac{\phi_R(p, t)}{\alpha(p)} + \frac{\phi_I(p, t)}{\beta(p)} \right\}. \tag{4.17b}$$

Notice that $\phi_1(p,t)$ becomes deterministic. It reflects the fact that we adopted the simplest definition for ξ in which only one gaussian white noise is needed (see eq. (4.7)), and it is consistent with the appearance of the δ-function in the distribution (4.12). Since ϕ_1 clearly converges in the limit $t \to \infty$, we should investigate whether the stochastic process $\phi_2(p,t)$ described in eq. (4.16b) has a unique equilibrium distribution.

The Fokker–Planck equation equivalent to eq. (4.16b) is expressed with a Fokker–Planck hamiltonian

$$H_{\mathrm{FP}}[\phi_2] = -2\int \mathrm{d}^4p \, \frac{\delta}{\delta\phi_2}\left(\frac{\delta}{\delta\phi_2(-p)} + \frac{\delta S_{\mathrm{eff}}[\phi_2]}{\delta\phi_2(-p)}\right), \tag{4.18a}$$

where

$$S_{\mathrm{eff}}[\phi_2] = \int \mathrm{d}^4p \, \frac{A(p)}{2}\phi_2(-p)\phi_2(p). \tag{4.18b}$$

Performing a similarity transformation using an operator

$$V[\phi_2] = \mathrm{e}^{(1/2)S_{\mathrm{eff}}[\phi_2]}, \tag{4.19}$$

the hamiltonian becomes

$$H_{\mathrm{FP}}^V = VH_{\mathrm{FP}}V^{-1} = \int \mathrm{d}^4p \, 2\hat{a}^\dagger(p)\hat{a}(p), \tag{4.20}$$

with

$$\hat{a}(p) = -\frac{\delta}{\delta\phi_2(-p)} - \frac{1}{2}\frac{\delta S_{\mathrm{eff}}[\phi_2]}{\delta\phi_2(-p)}, \qquad \hat{a}(p)^\dagger = \frac{\delta}{\delta\phi_2(p)} - \frac{1}{2}\frac{\delta S_{\mathrm{eff}}[\phi_2]}{\delta\phi_2(p)}. \tag{4.21a,b}$$

Eq. (4.20) exhibits positive semi-definiteness of $H_{\mathrm{FP}}^V[\phi_2]$, i.e. of $H_{\mathrm{FP}}[\phi_2]$. This together with the assumption that $H_{\mathrm{FP}}[\phi_2]$ has a non-degenerate discrete ground state with eigenvalue zero guarantees the existence of a unique equilibrium distribution $P_{\mathrm{eq}}[\phi_{\mathrm{R}}, \phi_{\mathrm{I}}]$.

For other definitions of ξ in which two (or more) gaussian white noises are used, $\phi_1(p,t)$ does not become deterministic. In this case we can directly prove the positivity of $H_{\mathrm{FP}}[\phi_{\mathrm{R}}, \phi_{\mathrm{I}}]$ itself by diagonalizing it. For application to numerical simulation, such double-noise formulations would be more suitable since the definition can be given in the x-space.

5. The role of the kernel in the numerical approach to non-linear systems

The purpose of this section is to show the role of the kernel in the numerical approach to non-linear systems. As a prototype we first take for the action a simple power of x, $S \sim x^n$. Later we will extend the discussion to a polynomial form for the action S.

5.1. DISCUSSION OF THE SIMPLE POWER MODEL

In this subsection we would like to discuss the stability of the Langevin system with a kernel for a simple power model

$$S_n = \frac{\sigma}{n} x^n, \tag{5.1}$$

for the action with even n. The system is discussed with $\sigma = e^{i\phi}$ covering the whole complex σ-plane, i.e., $|\sigma| = 1$.

For this S_n the averages $\langle x^{2m} \rangle$, $m = 0, 1, 2, \ldots$ are calculated exactly for $\mathrm{Re}(\sigma) > 0$:

$$\langle x^{2m} \rangle = \left(\frac{n}{\sigma} \right)^{2m/n} \frac{\Gamma((2m+1)/n)}{\Gamma(1/n)} . \tag{5.2a}$$

The result can be analytically continued into the whole first Riemann sheet of σ, where the branch cut is taken along the negative imaginary axis, i.e.

$$-\pi < \mathrm{Arg}(\sigma) \equiv \phi_0 < \pi . \tag{5.2b}$$

This restriction on ϕ makes eq. (5.2a) unique. If this is not done, eq. (5.2a) gives the full $(n/2)$-fold set of solutions corresponding to σ in all Riemann sheets. As we have discussed previously, the physical interpretation of the above treatment for the model with $\mathrm{Re}(\sigma) \leqslant 0$ is not clear, however, analyzing such models will appear to be useful in an interpretation of the numerical results of complex Langevin simulation.

It is interesting to note that the Langevin equation with a phase rotating kernel is able to give the full set of solutions, at least in principle. The Langevin equation (2.1) becomes in this case

$$\dot{z} = -K\sigma z^{n-1} + \sqrt{K}\eta . \tag{5.3}$$

From now on the notation

$$\sigma_k = \sigma_0 e^{2\pi k i}, \quad k = 0, 1, 2, \ldots, \left(\tfrac{1}{2}n - 1\right) \tag{5.4}$$

is used to specify σ in the $(k+1)$th Riemann sheet. Our aim is to select that specific region of phases of K, for which the solution of the above equation is physical.

Dividing both sides of eq. (5.3) by $\sqrt{K}$ and rewriting it by introducing

$$r = K^{-1/2} z , \tag{5.5}$$

we get

$$\dot{r} = -K^{n/2} \sigma r^{n-1} + \eta . \tag{5.6}$$

Noting that η is taken to be real, a stable solution is guaranteed if the coefficient of the drift term is positive. From this argument we have $K^{n/2}\sigma = e^{0i} = 1$, i.e.,

$$K = \sigma^{-2/n} . \tag{5.7}$$

Therefore the stability region is not unique if $n > 2$ due to the fact that the function is multi-valued. Actually, if we replace σ by σ_k as defined in eq. (5.4) we get $n/2$ different values K_k,

$$K_k = (\sigma_0)^{-2/n} e^{-(4\pi/n)ki} , \tag{5.8}$$

all of which will be capable of stabilizing the original Langevin equation (5.3).

We want to show now that the different values of K_k will lead to the $n/2$-fold different solutions of (5.2a) with σ continued to the different Riemann sheets. In fact, recalling eq. (5.5), where r is real, the variety of K_k leads to a corresponding variety of solutions for z:

$$z_k = (\sigma_0)^{-1/n} e^{-(2\pi/n)ki} |z| = \left(\frac{1}{\sigma_k} \right)^{1/n} |z| , \tag{5.9}$$

where $|z| = r$ because of $|K| = 1$. This proves immediately our above statement.

To summarize, the phase rotating kernel can be divided into regions around the values

$$K_k = (\sigma_0)^{-2/n} e^{-(4\pi/n)ki} = e^{-(2/n)(\phi_0 + 2k\pi)i} . \tag{5.10a}$$

The *physical* result, however, is obtained from the above formula with $k = 0$, i.e., we have to choose the kernel in the region of

$$K \sim K_0 \tag{5.10b}$$

only. This choice ensures that we get the solution in the first Riemann sheet. Different choices of the kernel around $K \sim K_k$ with $k \neq 0$ will give also stable, however unphysical solutions. For the complex gaussian model treated in sect. 3 as an example we have $n = 2$ and therefore no branch cut, see eq. (5.2). In this case the

best choice for the kernel is

$$K = \sigma^{-1} = \sigma^*, \tag{5.11}$$

which is exactly that used in sect. 3. For $n = 4$ there exists one physical and one unphysical solution*, each of which is obtained from the Langevin equation with a kernel in the region

$$K_0 = (\sigma_0)^{-1/2}, \quad \text{and} \quad K_1 = (\sigma_0)^{-1/2} e^{-\pi i}. \tag{5.12}$$

Numerical results of this case are discussed below.

5.2. NUMERICAL RESULTS FOR THE CASE $n = 4$

This model has been investigated in a naïve Langevin simulation ($K = 1$) in ref. [5], where the conclusion was drawn, that it is difficult to penetrate into the region near to the imaginary axis in the complex σ-plane. We reinvestigate this model to show that the introduction of a kernel is really efficient in complex Langevin simulation, if we select carefully the physical solution as discussed above. We take the complex σ

$$\sigma = e^{(\pi/6)li}, \quad l = -6, \ldots, 6 \tag{5.13}$$

with a branch cut in $[-\infty, 0]$. For the numerical Langevin simulation we use a phase rotating kernel introduced in eq. (3.13), with discrete steps for the angle:

$$K = e^{-(\pi/24)Mi}, \quad M = 0, \ldots, 47. \tag{5.14}$$

Again a simple Euler discretization has been used with the time step $dt = 0.01$. A sample of 64 runs has been taken to estimate the error, with 2000 iterations for each run. In fig. 2 we show the case $l = 5$, where the naïve Langevin simulation completely fails, as a typical example. Fig. 2a shows the numerical results of z^2 for all M. One can see that the results calculated with values of M ranging from $M = 0, \ldots, 4$, $M = 16, \ldots, 28$ and $M = 40, \ldots, 47$ are distributed over the whole $\langle z^2 \rangle$-plane, while the results for those 10 values in between $M = 5$ and $M = 15$ are accumulated exactly at that point which also results from the analytic equation (5.2) with $n = 4$. These latter points are again shown in fig. 2b in a larger scale.

On the other hand, the kerneled Langevin equation picks also up the unphysical solution. It is clearly seen in fig. 2a that there exists another accumulation point for $M = 29, \ldots, 39$, which is around $K = \sigma^{-1/2} e^{-\pi i}$ as expected from the general discussion above. The calculated average of z^2 in this region has the opposite sign

* Unphysical solutions have also been found by Z. Bern [21].

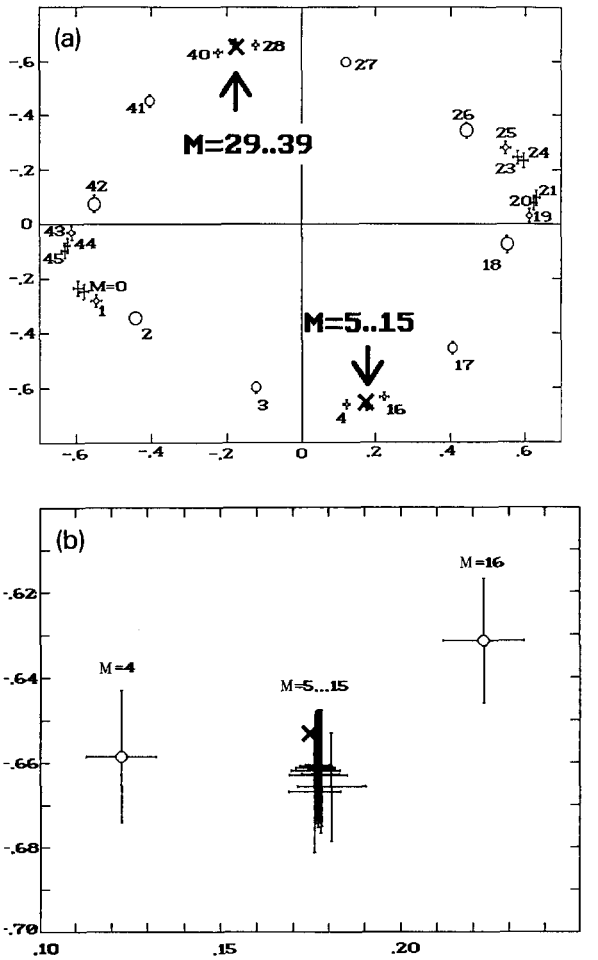

Fig. 2. (a) The average $\langle z^2 \rangle$ for an action $S = \sigma x^4/4$, with $\sigma = 5\pi i/6$. A phase rotating kernel $K = \exp\{-\pi M i/24\}$, $M = 0, \ldots, 47$, has been used in the simulation. Each point has been labelled by its corresponding value for M. The size of the circles corresponds to the number of blow-up solutions. The cross $\times$ denotes the exact solution. (b) Similar to (a), however, only the points $M = 4, \ldots, 16$ have been plotted in an enlarged scale.

of that obtained in the physical region and consistent with the analytic result (5.2a) with σ in the second Riemann sheet.

In fig. 2 the radius of the circles represents the number of blow-up solutions encountered. A blow-up solution has been defined in the following way: if during the update procedure $|z|$ becomes bigger than a certain value ($|z|_{\max} \sim 1000$), the run is rejected and replaced by a new one. The points in fig. 2 which are not accumulated, are accompanied by several blow-up solutions (up to ~ 100), while the accumulating points are free of them. In order to investigate the stability of the

situation represented in fig. 2b we have repeated the calculation reducing $|z|_{\max}$ to about 3, but the result did not change except that the number of blow-up solutions for the two points $M = 4$ and $M = 16$ increased. Thus at least in this simple model the number of blow-up solutions is a reliable probe to fix the phase of the kernel which leads to stable results.

Combining our theoretical insight discussed in sect. 5.1 and the numerical evidence discussed above we are in a position to give criteria how to select the physical solution: We define stable points as those which are free of blow-up solutions and which lie within the accumulation region. By taking only those stable points obtained with a kernel around K_0 in eq. (5.12) and throwing away unphysi-

TABLE 1a

Average $\langle z^2 \rangle$ calculated from a Langevin equation with $S = (\sigma/4)x^4$ and $\sigma = \exp\{(\pi/6)li\}$. The values calculated from eq. (5.3) are given in the second column. In the third column our results with stabilizing kernel are presented, while the last column gives the "naïve" results

	$\langle z^2 \rangle$		
l	exact	with kernel	naïve
−5	$0.175 + 0.653i$	$0.177 + 0.662i$ $\pm(0.002 + 0.004i)$	$-0.579 + 0.245i$ $\pm(0.012 + 0.026i)$
−4	$0.338 + 0.585i$	$0.343 + 0.594i$ $\pm(0.002 + 0.004i)$	$-0.338 + 0.443i$ $\pm(0.022 + 0.023i)$
−3	$0.478 + 0.478i$	$0.485 + 0.485i$ $\pm(0.003 + 0.003i)$	$0.435 + 0.509i$ $\pm(0.011 + 0.014i)$
−2	$0.585 + 0.338i$	$0.594 + 0.343i$ $\pm(0.004 + 0.002i)$	$0.594 + 0.343i$ $\pm(0.011 + 0.010i)$
−1	$0.653 + 0.175i$	$0.662 + 0.177i$ $\pm(0.004 + 0.002i)$	$0.661 + 0.176i$ $\pm(0.012 + 0.006i)$
0	$0.676 + 0.000i$	$0.685 + 0.000i$ $\pm(0.004 + 0.001i)$	$0.684 + 0.000i$ $\pm(0.013 + 0.00i)$
1	$0.653 - 0.175i$	$0.662 - 0.177i$ $\pm(0.004 + 0.002i)$	$0.661 - 0.176i$ $\pm(0.012 + 0.005i)$
2	$0.585 - 0.338i$	$0.593 - 0.343i$ $\pm(0.004 + 0.002i)$	$0.594 - 0.343i$ $\pm(0.011 + 0.010i)$
3	$0.478 - 0.478i$	$0.485 - 0.485i$ $\pm(0.003 + 0.003i)$	$0.435 - 0.509i$ $\pm(0.012 + 0.014i)$
4	$0.338 - 0.585i$	$0.343 - 0.594i$ $\pm(0.002 + 0.004i)$	$-0.337 - 0.443i$ $\pm(0.022 + 0.023i)$
5	$0.175 - 0.653i$	$0.177 - 0.662i$ $\pm(0.002 + 0.004i)$	$-0.580 - 0.245i$ $\pm(0.012 + 0.026i)$
6	$0.000 + 0.676i$	$0.000 + 0.686i$ $\pm(0.001 + 0.004i)$	$-0.635 - 0.072i$ $\pm(0.008 + 0.029i)$

cal stable points around K_1, we have calculated final averages for $\langle z^2 \rangle$ and $\langle z^4 \rangle$, which we give in table 1a, b. As can be seen from these tables, the introduction of the kernel has indeed improved the result appreciably, showing again the efficiency of the method.

In closing this section, we would like to comment on the numerical values presented in table 1. One might feel that these values show a small but persistent systematic deviation from the analytical ones, see also fig. 2b. The deviation, however, can be understood as a finite fictitious time step size effect. In order to check this statement, we have also used a second order discretization algorithm [22], while table 1 has been calculated by the simplest Euler type discretization of the

TABLE 1b

Average $\langle z^4 \rangle$ calculated from a Langevin equation with $S = (\sigma/4)x^4$ and $\sigma = \exp\{(\pi/6)li\}$. The values calculated from eq. (5.3) are given in the second column. In the third column our results with stabilizing kernel are presented, while the last column gives the "naïve" results

	$\langle z^4 \rangle$		
l	exact	with kernel	naïve
−5	$-0.866 + 0.500i$	$-0.892 + 0.515i$ $\pm(0.009 + 0.006i)$	$-0.907 + 0.515$ $\pm(0.030 + 0.031)$
−4	$-0.500 + 0.866i$	$-0.515 + 0.892i$ $\pm(0.006 + 0.009i)$	$-0.481 + 0.953$ $\pm(0.086 + 0.089)$
−3	$0.000 + 1.000i$	$0.000 + 1.030i$ $\pm(0.003 + 0.010i)$	$-0.002 + 1.045$ $\pm(0.026 + 0.036)$
−2	$0.500 + 0.866i$	$0.515 + 0.892i$ $\pm(0.006 + 0.009i)$	$0.522 + 0.891$ $\pm(0.013 + 0.033)$
−1	$0.866 + 0.500i$	$0.892 + 0.515i$ $\pm(0.009 + 0.006i)$	$0.893 + 0.511$ $\pm(0.026 + 0.020)$
0	$1.000 + 0.000i$	$1.030 - 0.000i$ $\pm(0.010 + 0.003i)$	$1.027 + 0.000$ $\pm(0.033 + 0.000)$
1	$0.866 - 0.500i$	$0.892 - 0.515i$ $\pm(0.009 + 0.006i)$	$0.893 - 0.511$ $\pm(0.026 + 0.020)$
2	$0.500 - 0.866i$	$0.515 - 0.892i$ $\pm(0.006 + 0.009i)$	$0.522 - 0.891$ $\pm(0.013 + 0.033)$
3	$0.000 - 0.100i$	$-0.000 - 1.031i$ $\pm(0.003 + 0.010i)$	$-0.002 - 1.045$ $\pm(0.026 - 0.036)$
4	$-0.500 - 0.866i$	$-0.515 - 0.892i$ $\pm(0.006 + 0.009i)$	$-0.481 - 0.953$ $\pm(0.086 + 0.089)$
5	$-0.866 - 0.500i$	$-0.892 - 0.515i$ $\pm(0.009 + 0.006i)$	$-0.908 - 0.516$ $\pm(0.030 + 0.031)$
6	$-1.000 + 0.000i$	$-1.030 + 0.000i$ $\pm(0.010 + 0.003i)$	

Langevin equation (2.1). As an example, we give the result for the case of $\sigma = \exp\{(5\pi/6)i\}$ obtained with the second order algorithm, $\langle z^2 \rangle = 0.175 - 0.654i$, which is very close to the exact value $\langle z^2 \rangle = 0.175 - 0.653i$. This has to be compared to the result obtained by the first order algorithm $\langle z^2 \rangle = 0.177 - 0.662i$. The same effect can be observed for other σ's.

5.3. DISCUSSION OF THE POLYNOMIAL MODEL FOR THE ACTION

The discussion of sect. 5.1 shall now be extended to the case of the more general action

$$S = \sum_{i=1}^{n} \frac{\sigma^{(2i)}}{2i} x^{2i}. \tag{5.15}$$

The corresponding Langevin equation with a kernel reads

$$\dot{z} = -K \sum_{i=1}^{n} \sigma^{(2i)} z^{2i-1} + \sqrt{K}\eta. \tag{5.16}$$

Introducing the variable r as defined in eq. (5.5), we obtain the Langevin equation in terms of r:

$$\dot{r} = -\sum_{i=1}^{n} K^i \sigma^{(2i)} z^{2i-1} + \eta. \tag{5.17}$$

In the previous sections for a simple power model we have arrived at the conclusion

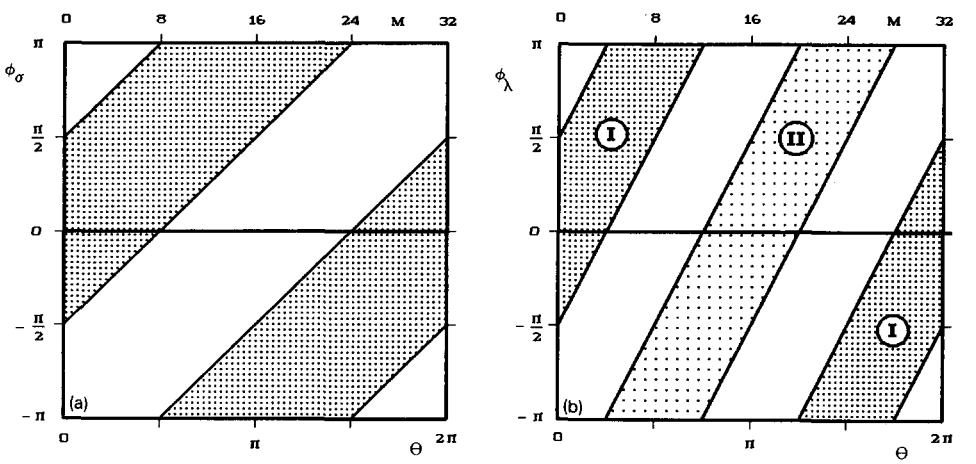

Fig. 3. (a) Convergence regions in the $[\phi_\sigma, \theta]$-plane for the simplified polynomial model discussed in subsect. 6.4. Shaded regions are those where convergence due to the σ-part is expected. (b) Convergence regions in the $[\phi_\lambda, \theta]$-plane for the simplified polynomial model discussed in subsect. 6.4. Shaded regions are those where convergence due to the λ-part is expected. The region labelled Π corresponds to a region of stability; however, in this region an unphysical solution is expected.

that $K^i\sigma^{(2i)} \approx e^{0i}$ will give us the physical stable solution. This argument can be applied to each term in eq. (5.17) separately, which leads us to the conjecture that the physical stability region is in this case given by

$$K^i\sigma^{(2i)} \approx e^{0i} \quad \text{or} \quad -\frac{\pi}{2} < \mathrm{Arg}(K^i\sigma^{(2i)}) < \frac{\pi}{2} \quad \text{for all } i. \tag{5.18}$$

We would like to mention that for a general model this is a quite severe restriction. It is possible that the Langevin system has stable solutions, for which the above condition is not fulfilled. In these cases the solutions are not physical ones, even if they are stable: they belong to the $\sigma^{(2i)}$'s in another Riemann sheet.

5.4. NUMERICAL RESULTS FOR A SIMPLIFIED POLYNOMIAL MODEL

To clarify these discussions we would like to consider in more detail the model

$$S = \frac{\sigma}{2}x^2 + \frac{\lambda}{4}x^4. \tag{5.19}$$

Referring to eq. (5.17), we notice that σ is rotated by K, while λ is rotated by K^2. Let us define the complex quantities

$$\sigma = e^{i\phi_\sigma}, \qquad \lambda = e^{i\phi_\lambda}, \qquad K = e^{-i\theta}. \tag{5.20}$$

In figs. 3a, b the shaded regions represent the expected convergence regions of $[\phi_\sigma, \theta]$ and $[\phi_\lambda, \theta]$, compare eq. (5.18). Note that in fig. 3b there is a region (labeled by "II"), where we expect convergence, however, the result will not be the physical

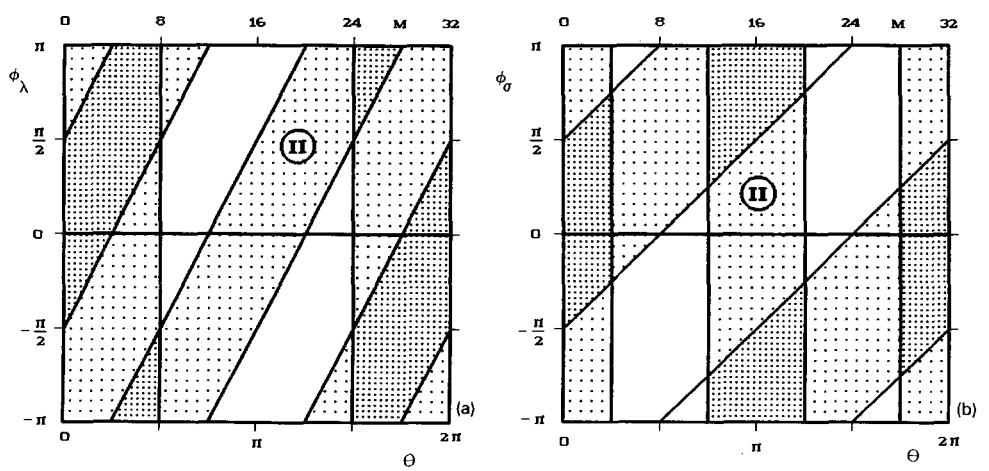

Fig. 4. (a) The overlapping region of convergence for $\sigma = 1$ while λ is taken complex. In the double shaded regions one expects convergent solutions. (b) Similar to (a), but with $\lambda = 1$ while σ is taken complex.

one, because λ is in the second Riemann sheet here. If the arguments of the complex σ and λ are given, the values for θ which gives physical results for simple power models ($S \propto \sigma x^2$ or $S \propto \lambda x^4$) can be extracted. The overlapping region, if it exists, will then determine the region for the kernel to be used in the full model.

To show how to use these figures in order to find the correct region for the kernel we discuss in more detail the model (i) for $\sigma = 1$ and λ complex, and (ii) for $\lambda = 1$ and σ complex.

(i) Fig. 4a is similar to fig. 3b, but we have indicated the regions where we expect stability from the σx^2-term obtained by taking $\phi_\sigma = 0$ in fig. 3a. We have solved the

TABLE 2
Average $\langle z^2 \rangle$ calculated from a Langevin equation with $S = (\sigma/2)x^2 + (\lambda/4)x^4$ with $\sigma = 1$ and $\lambda = \exp\{3(\pi/4)i\}$ for different values of the kernel $K = \exp\{-(\pi/16)Mi\}$

	$\lambda = \exp\{3(\pi/4)i\}$	
M	$\langle z^2 \rangle$	blow-up's
0	$0.2965 - 0.3644i$	20
1	$0.3855 - 0.4284i$	0
2	$0.3786 - 0.4030i$	0
3	$0.3794 - 0.4147i$	0
4	$0.3784 - 0.4125i$	0
5	$0.3763 - 0.4142i$	0
6	$0.3846 - 0.4296i$	0
7	$0.3697 - 0.4166i$	0
8	$0.3680 - 0.4147i$	0
9	$0.4088 - 0.3953i$	10
10	$0.8437 + 0.0938i$	156
11	$1.1028 + 0.7139i$	83
12	$1.1202 + 0.7450i$	1
13	$1.1431 + 0.7446i$	1
14	$1.1492 + 0.7352i$	10
15	$1.0782 + 0.8583i$	2
16	$1.0792 + 0.8367i$	1
17	$1.0843 + 0.8186i$	4
18	$0.9582 + 0.8797i$	117
19	$0.4554 + 0.9456i$	67
20	$0.0798 + 0.8529i$	15
21	$-0.0007 + 0.7815i$	0
22	$-0.0086 + 0.7726i$	0
23	$-0.0008 + 0.7645i$	1
24	$0.0038 + 0.7695i$	0
25	$0.0080 + 0.7609i$	0
26	$-0.0029 + 0.7560i$	0
27	$-0.0525 + 0.7088i$	23
28	$-0.1194 + 0.4436i$	45
29	$-0.1290 + 0.2543i$	29
30	$-0.0915 + 0.0807i$	33
31	$0.0477 - 0.1113i$	9

corresponding Langevin equation numerically changing ϕ_λ in steps of $\pi/4$, and θ in steps of $\pi/16$. Out of the data obtained we show the results for $\phi_\lambda = 3\pi/4$ in table 2 as a special example. From the double-shaded region at $\phi_\lambda = 3\pi/4$ in fig. 4a one expects a stable physical solution for $2 \leqslant M \leqslant 8$ and a stable unphysical solution for $24 \leqslant M \leqslant 26$. An inspection of table 2 shows a region of no blow-up solution for $1 \leqslant M \leqslant 8$ and from $21 \leqslant M \leqslant 26$. Predicted and calculated regions agree well. The restrictions due to the σx^2-term are less important than those due to the λx^4-term because it has a lower power than the other one. This explains the small deviations.

(ii) In this case fig. 4b applies, from which we can get the correct convergence regions as in the previous case. For $3\pi/4 < \phi_\sigma < \pi$ and $-\pi < \phi_\sigma < -3\pi/4$ there is no double shaded region within the first Riemann sheet for λ. In spite of that we get convergent results also here, however in a very restricted region of $M \sim 0$ and $M \sim 31$. This is the center of the convergence region for λ, which dominates the convergence property of the model as we discussed before. We would like to mention that we have $|\sigma| = |\lambda| = 1$ here. If, however, $|\sigma| \gg |\lambda|$ the dominance of λx^4 is weakened. Thus we might lose this stable solution in such a case. We did, e.g., not succeed in obtaining a physical stable solution in the case of $\lambda = 1$ and $\sigma = -0.5 + 2i$, while the unphysical solution was stable.

Using these criteria, we have extracted the final results from our data and compare them to "analytical" results: For $\mathrm{Re}(\lambda) > 0$ a direct numerical integration can be performed. In the other cases we mean by "analytical result" the analytical continuation of the perturbative calculation. In these cases the perturbation is performed in expanding $e^{-(\sigma/2)x^2}$:

$$\langle x^2 \rangle = \frac{\int dx\, x^2 e^{-(\sigma/2)x^2 - (\lambda/4)x^4}}{\int dx\, e^{-(\sigma/2)x^2 - (\lambda/4)x^4}} = \frac{4\sqrt{\lambda}\, N_1 \Gamma\left(\frac{3}{4}\right) - \sigma N_2 \Gamma\left(\frac{1}{4}\right)}{-2\sqrt{\lambda}\,\sigma D_1 \Gamma\left(\frac{3}{4}\right) + 2\lambda D_1 \Gamma\left(\frac{1}{4}\right)}. \quad (5.21)$$

The abbreviations N_1, N_2, D_1, D_2 in this equation are given, with $\kappa = \sigma^2/4\lambda$, by

$$N_1 \equiv \sum_{n=1}^{\infty} \frac{\kappa^n}{(2n)!} \prod_{i=1}^{n} (4i-1), \qquad N_2 \equiv \sum_{n=0}^{\infty} \frac{\kappa^n}{(2n+1)!} \prod_{i=0}^{n} (4i+1),$$

$$D_1 \equiv \sum_{n=1}^{\infty} \frac{\kappa^n}{(2n+1)!} \prod_{i=1}^{n} (4i-1), \qquad D_2 \equiv \sum_{n=1}^{\infty} \frac{\kappa^n}{(2n)!} \prod_{i=1}^{n} (4i-3). \quad (5.22)$$

The expansion on the r.h.s. of eq. (5.21) is meaningful only in the case of $\mathrm{Re}(\lambda) > 0$, but the result can be continued into the whole complex plane. The physical results are obtained by taking λ within the first Riemann sheet, while λ from the second sheet gives the unphysical ones.

The final results are presented in tables 3a and 3b. We have also included the results of similar calculations for $\sigma = i$ and $\lambda = i$, respectively, in tables 4a and 4b.

TABLE 3a
Average $\langle z^2 \rangle$ calculated from a Langevin equation with $S = (\sigma/2)x^2 + (\lambda/4)x^4$ with $\sigma = 1$ and $\lambda = \exp\{(\pi/4)li\}$

l	$\langle z^2 \rangle$		
	exact	with kernel	naïve
−3	$0.381 + 0.418i$	$0.378 + 0.417i$ $\pm(0.004 + 0.006i)$	$0.292 + 0.371i$ $\pm(0.005 + 0.009i)$
−2	$0.438 + 0.260i$	$0.434 + 0.259i$ $\pm(0.005 + 0.004i)$	$0.430 + 0.245i$ $\pm(0.004 + 0.004i)$
−1	$0.461 + 0.124i$	$0.460 + 0.124i$ $\pm(0.005 + 0.003i)$	$0.458 + 0.122i$ $\pm(0.005 + 0.002i)$
0	$0.468 + 0.000i$	$0.465 - 0.000i$ $\pm(0.005 + 0.002i)$	$0.468 + 0.000i$ $\pm(0.005 + 0.000i)$
1	$0.461 - 0.124i$	$0.456 - 0.124i$ $\pm(0.005 + 0.002i)$	$0.461 - 0.123i$ $\pm(0.004 + 0.002i)$
2	$0.438 - 0.260i$	$0.435 - 0.260i$ $\pm(0.005 + 0.004i)$	$0.441 - 0.257i$ $\pm(0.004 + 0.005i$
3	$0.381 - 0.418i$	$0.378 - 0.417i$ $\pm(0.004 + 0.006i)$	$0.297 - 0.364i$ $\pm(0.005 + 0.009i)$
4	$0.256 - 0.601i$	$0.252 - 0.597i$ $\pm(0.003 + 0.008i)$	

TABLE 3b
Average $\langle z^2 \rangle$ calculated from a Langevin equation with $S = (\sigma/2)x^2 + (\lambda/4)x^4$ with $\lambda = 1$ and $\sigma = \exp\{(\pi/4)ni\}$

n	$\langle z^2 \rangle$		
	exact	with kernel	naïve
0	$0.468 + 0.000i$	$0.465 - 0.000i$ $\pm(0.005 + 0.002i)$	$0.468 + 0.000i$ $\pm(0.005 + 0.000i)$
1	$0.493 - 0.126i$	$0.490 - 0.124i$ $\pm(0.006 + 0.002i)$	$0.492 - 0.123i$ $\pm(0.005 + 0.002i)$
2	$0.601 - 0.256i$	$0.588 - 0.251i$ $\pm(0.008 + 0.003i)$	$0.587 - 0.246i$ $\pm(0.007 + 0.004i)$
3	$0.855 - 0.280i$	$0.851 - 0.275i$ $\pm(0.010 + 0.003i)$	$0.857 - 0.275i$ $\pm(0.010 + 0.005i)$
4	$1.042 + 0.000i$	$1.031 - 0.005i$ $\pm(0.011 + 0.002i)$	$1.032 - 0.000i$ $\pm(0.011 + 0.000i)$
5	$0.855 + 0.280i$	$0.838 + 0.273i$ $\pm(0.010 + 0.004i)$	$0.843 + 0.271i$ $\pm(0.011 + 0.005i)$
6	$0.601 + 0.256i$	$0.593 + 0.250i$ $\pm(0.007 + 0.003i)$	$0.588 + 0.248i$ $\pm(0.008 + 0.004i)$
7	$0.493 + 0.126i$	$0.492 + 0.126i$ $\pm(0.006 + 0.002i)$	$0.482 + 0.122i$ $\pm(0.006 + 0.002i)$

TABLE 4a
Average $\langle z^2 \rangle$ calculated from a Langevin equation with $S = (\sigma/2)x^2 + (\lambda/4)x^4$ with $\sigma = i$ and $\lambda = \exp\{(\pi/4)li\}$

	$\langle z^2 \rangle$		
l	exact	with kernel	naïve
−3	$0.539 + 0.846i$	$0.533 + 0.837i$ $\pm(0.005 + 0.010i)$	$-0.014 + 0.712i$ $\pm(0.009 + 0.013i)$
−2	$0.803 + 0.406i$	$0.786 + 0.395i$ $\pm(0.008 + 0.007i)$	$0.758 + 0.440i$ $\pm(0.010 + 0.008i)$
−1	$0.771 - 0.003i$	$0.757 - 0.003i$ $\pm(0.009 + 0.004i)$	$0.757 - 0.000i$ $\pm(0.009 + 0.003i)$
0	$0.601 - 0.256i$	$0.597 - 0.251i$ $\pm(0.008 + 0.003i)$	$0.603 - 0.255i$ $\pm(0.007 + 0.004i)$
1	$0.418 - 0.381i$	$0.411 - 0.376i$ $\pm(0.005 + 0.004i)$	$0.419 - 0.381i$ $\pm(0.006 + 0.007i)$
2	$0.260 - 0.438i$	$0.258 - 0.434i$ $\pm(0.004 + 0.005i)$	$0.186 - 0.446i$ $\pm(0.009 + 0.008i)$
3	$0.124 - 0.461i$	$0.124 - 0.459i$ $\pm(0.003 + 0.005i)$	$-0.953 + 0.207i$ $\pm(0.012 + 0.013i)$
4	$0.000 - 0.468i$	$-0.000 - 0.465i$ $\pm(0.002 + 0.005i)$	$-0.568 - 0.657i$ $\pm(0.005 + 0.015i)$

TABLE 4b
Average $\langle z^2 \rangle$ calculated from a Langevin equation with $S = (\sigma/2)x^2 + (\lambda/4)x^4$ with $\lambda = i$ and $\sigma = \exp\{(\pi/4)ni\}$

	$\langle z^2 \rangle$		
n	exact	with kernel	naïve
0	$0.438 - 0.260i$	$0.432 - 0.257i$ $\pm(0.005 + 0.004i)$	$0.440 - 0.257i$ $\pm(0.004 + 0.005i)$
1	$0.331 - 0.331i$	$0.328 - 0.328i$ $\pm(0.004 + 0.004i)$	$0.335 - 0.326i$ $\pm(0.003 + 0.006i)$
2	$0.260 - 0.438i$	$0.259 - 0.436i$ $\pm(0.004 + 0.005i)$	$0.191 - 0.438i$ $\pm(0.010 + 0.008i)$
3	$0.244 - 0.606i$	$0.243 - 0.599i$ $\pm(0.005 + 0.007i)$	$-0.690 - 0.999i$ $\pm(0.014 + 0.007i)$
4	$0.406 - 0.803i$	$0.408 - 0.797i$ $\pm(0.007 + 0.008i)$	$-0.255 - 1.224i$ $\pm(0.013 + 0.007i)$
5	$0.737 - 0.737i$	$0.726 - 0.727i$ $\pm(0.008 + 0.008i)$	$0.440 - 0.928i$ $\pm(0.013 + 0.009i)$
6	$0.803 - 0.406i$	$0.789 - 0.402i$ $\pm(0.009 + 0.006i)$	$0.774 - 0.423i$ $\pm(0.010 + 0.009i)$
7	$0.606 - 0.244i$	$0.602 - 0.242i$ $\pm(0.007 + 0.005i)$	$0.607 - 0.242i$ $\pm(0.006 + 0.006i)$

TABLE 5
Average $\langle z^2 \rangle$ calculated from a Langevin equation with $S = (\sigma/2)x^2 + (\lambda/4)x^4$ with $\lambda = 0.1$ and $\sigma = \exp\{(\pi/4)ni\}$

n	$\langle z^2 \rangle$		
	exact	with kernel	naïve
0	$0.818 + 0.000i$	$0.802 - 0.000i$ $\pm(0.014 + 0.000i)$	$0.811 + 0.000i$ $\pm(0.014 + 0.000i)$
1	$0.766 - 0.487i$	$0.750 - 0.482i$ $\pm(0.004 + 0.003i)$	$0.763 - 0.483i$ $\pm(0.014 + 0.012i)$
2	$0.469 - 1.310i$	$0.481 - 1.247i$ $\pm(0.011 + 0.012i)$	$0.998 - 1.969i$ $\pm(0.034 + 0.097i)$
3	$2.144 - 6.408i$		$6.052 - 5.935i$ $\pm(0.060 + 0.080i)$
4	$8.704 + 0.000i$	$8.118 + 0.008i$ $\pm(0.045 + 0.009i)$	$8.040 - 0.001i$ $\pm(0.091 + 0.002i)$
5	$2.144 + 6.408i$		$5.981 + 5.942i$ $\pm(0.062 + 0.069i)$
6	$0.469 + 1.310i$	$0.480 + 1.241i$ $\pm(0.010 + 0.013i)$	$0.956 + 1.728i$ $\pm(0.032 + 0.087i)$
7	$0.766 + 0.487i$	$0.747 + 0.472i$ $\pm(0.004 + 0.003i)$	$0.763 + 0.483i$ $\pm(0.014 + 0.012i)$

All the data with suitably chosen kernels agree well with those calculated analytically, while the "naïve" results ($K \equiv 1$) in certain cases show appreciable deviations. This proves our claim that the complex Langevin simulation is complete only with the introduction of a kernel whose stability region is correctly adjusted. Naïve results (i.e., $K = 1$) are not always reliable.

The Langevin equation with a kernel can, however, also fail sometimes. If there is no overlapping region of convergence and the λx^4-term does not dominate as discussed in (ii), this happens. To show such a situation we have added table 5 where we have taken a fairly small value for λ compared to $|\sigma| = 1$, i.e. $\lambda = 0.1$. For $\phi_\sigma = \pm 3\pi/4$, we could not find stable physical results. Also we can see that the naïve results are not stable, because they depend severely on the kernel. On the other hand, for $\sigma = \pm i$ the introduction of a kernel refines the results appreciably, as expected.

6. Conclusion

As we mentioned in the introduction, there are two known reasons which mainly cause the failure of the complex Langevin simulation: The problem of (a) the blow-up solutions [7, 8], and (b) the segregation effect [9]. Up to now nobody knows whether both of them might be correlated or not.

In this paper we have discussed the role of the kernel in the complex Langevin equation, especially in connection with the problem of (a) above. We got the results: (i) The kernel which changes the eigenvalue spectrum of the Fokker–Planck hamiltonian can be adjusted to stabilize the system. The mechanism how this works is discussed through solving the Fokker–Planck equation in the simplest case. (ii) The result described in (i) shows that it is possible to control the convergence of stochastic quantization of the Minkowski action and of the bottomless action (e.g., linearized euclidean gravity) at least in the perturbative sense. (iii) Through the numerical simulation of very simple non-linear models in zero-dimensional field theory, we have checked the importance of a kernel in a complex Langevin equation. If the quantum mechanical average of a certain physical quantity is a multi-valued function of the parameter in the action, the kerneled Langevin equation gives the results in all branches. We give criteria to choose the kernel which leads to the physical result, or we can give criteria to exhibit a situation where no physical stable solution is expected.

On the other hand many points still remain which should be clarified in future studies. In numerical simulation, we have restricted our discussions to simple zero-dimensional field theoretical models. It is not a priori clear what kind of kernel can settle the convergence problem without being bothered with unphysical solutions in the case of more complicated problems in full field theories. However, we think that the precise knowledge obtained here from the analysis of simple models will surely be helpful for future work. Concerning the problem of segregation phenomena (b), it is an interesting question whether the kernel's degree of freedom can refine the situation. It is, e.g., known that the complex Langevin simulation of the system given by $S = \beta \cos\theta + \ln\tan\theta$ can well reproduce the correct results for $\langle \cos\theta \rangle$ in the weak coupling (large β) region, however, it fails completely in the strong coupling region because of the segregation effect [9, 23]. We have repeated the simulation of this system by introducing the phase rotating kernel. We could, however, not observe any refinement of the situation in the strong coupling region. Based on these observations, we feel that a further investigation of the problem should include an implementation of the idea of a field dependent kernel.

Finally we would like to state a conjecture about the relation between the number of blow-up solutions of a Langevin equation with a kernel and the positivity of the corresponding Fokker–Planck hamiltonian: The definition of a blow-up solution might in general depend on parameters like the allowed maximal value for $|z|$, the fictitious time step chosen, and the total number of updates. Choosing these parameters properly, in rotating the phase of the kernel we find regions of blow-up solutions and regions with no blow-up solutions, compare, e.g., table 2. Whenever we find a region of no blow-up solutions in those physical regions predicted from the discussion in sects. 5.3 and 5.4, we find a correct physical result. From this we might conclude that for those kernels the real part of the corresponding Fokker–Planck hamiltonian becomes positive. On the other hand, if one cannot find

such a region for the kernel, the result one obtains will always deviate from the correct one. Similar arguments have been given for the case of a naïve complex Langevin equation with $K = 1$ [24].

Appendix

To solve the Fokker–Planck equation for the complex gaussian model in eq. (3.7) we introduce the integration kernel $\mathscr{K}(x, y; x', y' : t)$ by

$$P(x, y : t) = \int \mathrm{d}x' \mathrm{d}y' \mathscr{K}(x, y; x', y' : t) P_0(x', y'), \tag{A.1}$$

where $P_0(x, y)$ is the initial distribution. From the Fokker–Planck equation (3.7) we get

$$\dot{\mathscr{K}}(x, y; x', y' : t) = -H_{\mathrm{FP}}(x, y)\, \mathscr{K}(x, y; x', y' : t), \tag{A.2a}$$

with the initial condition

$$\mathscr{K}(x, y; x', y' : 0) = \delta(x - x')\delta(y - y'). \tag{A.2b}$$

The formal solution of this equation is given by

$$\mathscr{K}(x, y; x', y' : t) = \mathrm{e}^{-H_{\mathrm{FP}}(x, y)t}\delta(x - x')\delta(y - y'), \tag{A.3}$$

which can be rewritten as

$$\begin{aligned}\mathscr{K}(x, y; x', y' : t) &= \delta\big(x - \phi_x(x', y' : t)\big)\delta\big(y - \phi_y(x', y' : t)\big) \\ &= \left(\frac{1}{2\pi}\right)^2 \int \mathrm{d}r\,\mathrm{d}s\, \mathrm{e}^{ir[x - \phi_x(x', y' : t)]}\, \mathrm{e}^{is[y - \phi_y(x', y' : t)]},\end{aligned} \tag{A.4}$$

where

$$\phi\begin{pmatrix} x \\ y \end{pmatrix}(x', y') = \mathrm{e}^{-H^\dagger(x', y')t}\begin{pmatrix} x \\ y \end{pmatrix}\mathrm{e}^{+H^\dagger(x', y')t}. \tag{A.5}$$

In this equation we have introduced the adjoint of the Fokker–Planck hamiltonian defined by

$$H^\dagger_{\mathrm{FP}}(x, y) = \alpha^2 \frac{\partial^2}{\partial x^2} + \beta^2 \frac{\partial^2}{\partial y^2} + 2\alpha\beta \frac{\partial^2}{\partial x\, \partial y} - (Ax - By)\frac{\partial}{\partial x} - (Bx + Ay)\frac{\partial}{\partial y}. \tag{A.6}$$

In order to get a closed form for the differential equations for the $\phi_{x,y}$ we define the generalized derivatives $D_{x,y}$ similarly to eq. (A.5)

$$D\binom{x}{y}(x', y') = \mathrm{e}^{-H^{\dagger}(x', y')t}\begin{pmatrix} \partial/\partial x \\ \partial/\partial y \end{pmatrix}\mathrm{e}^{+H^{\dagger}(x', y')t}, \tag{A.7}$$

and get

$$\dot{\phi}_x = 2\alpha^2 D_x + 2\alpha\beta D_y - A\phi_x + B\phi_y, \tag{A.8a}$$

$$\dot{\phi}_y = 2\alpha\beta D_x + 2\beta^2 D_y - B\phi_x - A\phi_y, \tag{A.8b}$$

$$\dot{D}_x = AD_x + BD_y, \qquad \dot{D}_y = -BD_x + AD_y. \tag{A.9a, b}$$

We have solved this set of equations using the initial condition $\phi_x(x, y:0) = x$, $\phi_y(x, y:0) = y$, $D_x(x, y:0) = \partial_x$, $D_y(x, y:0) = \partial_y$. The result is

$$\phi_x = E_1 x + E_2 y + F_1\,\partial_x + F_2\,\partial_y, \tag{A.10a}$$

$$\phi_y = E_3 x + E_4 y + F_3\,\partial_x + F_4\,\partial_y, \tag{A.10b}$$

with coefficients

$$E_1 = \mathrm{e}^{-At}\cos(Bt), \qquad E_2 = \mathrm{e}^{-At}\sin(Bt),$$

$$E_3 = -\mathrm{e}^{-At}\sin(Bt), \qquad E_4 = \mathrm{e}^{-At}\cos(Bt), \tag{A.11}$$

$$F_1 = u\sinh(At)\cos(Bt) - v\cosh(At)\sin(Bt) + w\sinh(At)\cos(Bt), \tag{A.12a}$$

$$F_2 = v\sinh(At)\cos(Bt) + u\cosh(At)\sin(Bt) + w\sinh(At)\sin(Bt), \tag{A.12b}$$

$$F_3 = v\sinh(At)\cos(Bt) + u\cosh(At)\sin(Bt) - w\sinh(At)\sin(Bt), \tag{A.12c}$$

$$F_4 = -u\sinh(At)\cos(Bt) + v\cosh(At)\sin(Bt) + w\sinh(At)\cos(Bt), \tag{A.12d}$$

where u, v and w have been defined in eq. (3.10).

In order to get the final form of $\mathscr{K}$ we have to perform the integration over r and s in eq. (A.4). Since $\phi_{x,y}$ contains derivatives, see eq. (A.10), one has to perform them by using the Baker–Campbell–Hausdorff formula first. We then get

$$\mathscr{K}(x, y; x', y':t) = \left(\frac{1}{2\pi}\right)^2 \int_{-\infty}^{\infty} \mathrm{d}r\,\mathrm{d}s \exp\left\{-\frac{r^2}{2}G_1 - rsG_2 - \frac{s^2}{2}G_3 - rH_1 - sH_2\right\}, \tag{A.13}$$

with

$$G_1 = E_1F_1 + E_2F_2, \qquad G_2 = E_3F_1 + E_4F_2, \qquad G_3 = E_3F_3 + E_4F_4. \quad \text{(A.14)}$$

The practical form of G_i and H_i is given in eq. (3.9) in the text.

After performing the Gauss integration over r and s we arrive at the final form for $\mathscr{K}$, from which we get, using eq. (3.8), the final form for the Fokker–Planck distribution.

References

[1] C. Peterson and L. Sköld, Nucl. Phys. B255 (1985) 365
[2] P. Hasenfratz and F. Karsch, Phys. Lett. B125 (1983) 308
[3] G. Bhanot, E. Rabinovici, N. Seiberg and P. Woit, Nucl. Phys. B230 [FS10] (1984) 291
[4] J. Ambjørn and S.-K. Yang, Nucl. Phys. B275 [FS17] (1986) 18
[5] G. Parisi, Phys. Lett. B131 (1983) 393
[6] J.R. Klauder, Phys. Rev. A29 (1984) 2036
[7] J.R. Klauder and W.P. Petersen, J. Stat. Phys. 39 (1985) 53
[8] J. Ambjørn and S.-K. Yang, Phys. Lett. B165 (1985) 140
[9] J. Flower, S.W. Otto and S. Callahan, Phys. Rev. D34 (1986) 598
[10] R.W. Haymaker and J. Wosiek, Phys. Rev. D34 (1986) 969
[11] J.D. Breit, S. Gupta and A. Zaks, Nucl. Phys. B233 (1984) 61;
P.H. Damgaard and K. Tsokos, Nucl. Phys. B235 [FS11] (1984) 75
[12] G. Parisi, Progress in gauge field theory, ed. G. 't Hooft, J. Jaffe, H. Lehmann, P.K. Mitter, I.N. Singer and R. Stora (Plenum, New York, 1984) p. 531;
G.G. Batrouni, G.R. Katz, A.S. Kronfeld, G.P. Lepage, B. Svetitsky and K.G. Wilson, Phys. Rev. D32 (1985) 2736
[13] B. Söderberg, Nucl. Phys. B295 [FS21] (1988) 396
[14] H. Hüffel and P.V. Landshoff, Nucl. Phys. B260 (1985) 545
[15] J. Sakamoto, Prog. Theor. Phys. 80 (1988) 190
[16] S.W. Hawking, Phys. Rev. D18 (1978) 1747;
G.W. Gibbons, S.W. Hawking and M.J. Perry, Nucl. Phys. B138 (1978) 141
[17] M. Namiki, Delta function and differential equations (Iwanami Publisher, Tokyo 1982) [in Japanese]
[18] H. Hüffel and H. Rumpf, Phys. Lett. B148 (1984) 104;
E. Gozzi, Phys. Lett. B150 (1985) 119
[19] H. Nakazato and Y. Yamanaka, Phys. Rev. D34 (1986) 492;
H. Nakazato, Prog. Theor. Phys. 77 (1987) 20
[20] D.J.E. Callaway, F. Cooper, J.R. Klauder and H.A. Rose, Nucl. Phys. B262 (1985) 19
[21] Z. Bern, private communication
[22] I.T. Drummond, S. Duane and R.R. Horgan, Nucl. Phys. B220 [FS58] (1983) 119
[23] J. Ambjørn, M. Flensburg and C. Peterson, Nucl. Phys. B275 [FS17] (1986) 375
[24] T. Matsui and A. Nakamura, Phys. Lett. B194 (1987) 262